Relationship Between Thrombolytic Therapy and Perfusion Defect Detected by Gd-DTPA–Enhanced Fast Magnetic Resonance Imaging in Acute Myocardial Infarction

Sadako Motoyama,[1] Takeshi Kondo,[1] Hirofumi Anno,[2]
Taika Kizukuri,[2] Yu Nakamura,[1] Keita Oshima,[1]
Takahisa Sato,[1] Masayoshi Sarai,[1] Hiroshi Kurokawa,[1]
Yoshihiko Watanabe,[1] and Hitoshi Hishida[1]

[1]Department of Cardiology and [2]Department of Radiology, Fujita
Health University, Toyoake, Japan

ABSTRACT

To study whether thrombolytic therapy affects Gd-DTPA–enhanced pattern and whether its pattern indicates myocardial viability, Gd-DTPA–enhanced magnetic resonance imaging (MRI) was performed in 43 patients with reperfused acute myocardial infarction 14.8 ± 5.0 days after onset with breathhold scanning on a 1.5-T whole body system. The hypoenhanced area at 90 sec after contrast injection was defined as a perfusion defect (PD). Patients were divided into PD(+) and PD(−) groups. The PD was detected in 77.8% of patients treated with direct percutaneous transluminal coronary angioplasty (PTCA) and in 28.6% of patients treated by thrombolytic therapy with or without PTCA in the thrombolysis in myocardial infarction grade 3 group (p < 0.05). The myocardial wall was divided into seven segments based on the American Heart Association committee report. Wall motion of each segment was classified by one of six patterns (wall motion score [WMS]: dyskinesis, −1; akinesis, 0; severe hypokinesis, 1; hypokinesis, 2; slight hypokinesis, 3; normal, 4). By echocardiography, the average WMS and ejection fraction were similar between the PD(+) group and the PD(−) group on admission. Those parameters were significantly worse in the PD(+) group than in PD(−) group 1 month

Address correspondence and reprint requests to Sadako Motoyama.

after onset. The change in WMS was significantly lower in the PD(+) group than in the PD(−) group. The number of patients and segments with more than two grades of improvement of WMS in the PD(+) group was significantly lower than that in the PD(−) group. Angiographically, left ventricular ejection fraction and WMS of the PD(+) group were significantly lower than those of the PD(−) group 3 months later. PDs were detected significantly less frequently in patients treated with thrombolytic therapy, suggesting that microvascular embolization related to formation of the no-reflow phenomenon.

***Key Words:** Acute myocardial infarction; Contrast-enhanced MRI; No-reflow phenomenon; Thrombolysis; Viability*

INTRODUCTION

Over the past several years, a number of experimental studies have suggested that contrast-enhanced magnetic resonance imaging (MRI) could be used to characterize microvascular perfusion (1–11). Early studies using spin echo imaging required several minutes to obtain each image of the heart (4–8). More recently, several groups used fast MRI to characterize the myocardial first pass of MR contrast agents after bolus administration (2,9–12). In a canine model, MRI hypoenhanced regions are characterized by profoundly reduced blood flow, with 90% of the myocardium nonviable (13). MRI hypoenhanced regions are also seen in humans, and these regions correlate with poorer global left ventricular function (14,15) and more frequent postmyocardial infarction complications (9,15). Therefore, the extent of hypoenhancement has important prognostic significance after acute myocardial infarction. We studied whether thrombolytic therapy has an effect on Gd-DTPA enhancement pattern.

MATERIALS AND METHODS

The study group consisted of 43 consecutive patients (37 men and 6 women, mean age, 59 ± 11 years) with reperfused acute myocardial infarction. Twenty-six patients suffered from anteroseptal myocardial infarction, 9 had inferior myocardial infarctions, and 8 had posterior myocardial infarctions. Gd-DTPA–enhanced MRI was performed 14.8 ± 5.0 days after myocardial infarction onset on a 1.5-T whole body system (Shimazu). T2-weighted images were acquired in vertical LV longitudinal sections to determine infarct location. High signal intensity area was seen in infarcted area on those T2-weighted images. A single short-axis slice including the infarct zone was chosen using those T2-weighted vertical LV longitudinal images. Gd-DTPA (0.2 mmol/kg) was injected for 20 sec by hand. Images were then acquired 30, 60, and 90 sec and 7 min after injection at this slice location. An LV short-axis slice image was obtained with use of a flip angle of 25 degrees, an echo time of 4.7 ms, repetition time of 11–14 msec, inversion recovery time of 400–500 msec, segmentation of seven to nine, one number of excitation, a field of view of 30 cm, and matrix of 109 × 256 or 163 × 256 in almost all patients. The flip angle and echo time were changed to obtain the optimal images in some patients, and Tl, segmentation, and matrix size were changed because of patient's R-R interval and breathhold period variability. Two observers analyzed the images.

Three patterns of myocardial signal enhancement were identified, as described earlier (11,13). In noninfarcted myocardium, signal intensity rose rapidly during the first 30 sec after contrast injection and then decayed over 7 min. Infarcted myocardium generated a signal that also rapidly rose in intensity during the first 90 sec after contrast injection. This caused hyperenhancement of infarcted myocardium relative to normal myocardium by 7 min after contrast injection. The third pattern was a gradual increase in signal intensity over the first 90 sec after contrast injection. Such areas are hypoenhanced relative to surrounding myocardium and correspond to regions of microvascular obstruction or ''no reflow'' (9–11, 13,16,17). Hypoenhancement persisted for 90 sec and was located in the subendocardium of the infarct core. The hypoenhancement area at 90 sec surrounded by the hyperenhanced area at 7 min after contrast injection was defined as perfusion defect (PD). Patients were divided into two groups, PD(+) and PD(−).

The infarcted area at 7 min after contrast injection was not estimated quantitatively. The short-axis slice of the infarcted zone did not seem to provide enough data to quantitatively calculate the infarcted area.

The study took 1.5 hr to get images, so long that we did not get fast echo cine. Additionally, MRI was performed about 2 weeks after the onset; therefore, it was not appropriate to compare the LV function in the acute phase with that in the chronic phase.

Emergent coronary angiography (CAG) was per-

formed. The occluded coronary artery was reperfused by means of percutaneous transluminal coronary angioplasty (PTCA) or thrombolytic therapy using tissue plasminogen activator. Although the first choice was direct PTCA for acute myocardial infarction, some patients were injected with tissue plasminogen activator in other hospitals before admission to our hospital or after PTCA. Because this is a retrospective study, selection of reperfusion therapy did not depend on sex, age, infarct size, or interval from onset to admission. The degree of success of thrombolysis in myocardial infarction (TIMI) (18) after reperfusion was evaluated and graded.

Two-dimensional echocardiography (Toshiba) was performed to evaluate LV function on admission and 1 month after onset. Restudy CAG and left ventriculography (LVG) were done 3 months after onset. Echocardiography studies were omitted at 3 months. To assess the LV function in the acute phase, echocardiography was used instead of LVG, which would cause an overload on the left ventricle. LVG was performed at 3 months with restudy CAG, so that echocardiography could be omitted. Many studies support that echocardiographic LV wall motion assessment is similar to LVG (19–21).

To assess the LV contraction by echocardiography and LVG by the same criteria, the images of the LV wall were divided into seven segments based on the American Heart Association committee report (22). Wall motion of the each segment was classified by six patterns and given a wall motion score (WMS) (dyskinesis, −1; akinesis, 0; severe hypokinesis, 1; hypokinesis, 2; slight hypokinesis, 3; normal, 4). Left ventricle four-chamber and two-chamber views were used to assess WMS by echocardiography. The total WMS of the seven segments was calculated. The number of segments that showed improvement of more than two grades of WMS and the number of patients who had more than two grades of improvement of WMS were obtained by echocardiography. The change in WMS was calculated by subtracting WMS on admission from the one obtained at 1 month after onset. The number of akinetic segments, by both echocardiography and LVG, was calculated.

LV ejection fraction (LVEF) was evaluated by echocardiography using the modified Simpson method and by LVG using the centerline method. Serum creatine kinase (CK)-MB was measured every 4 hr for at least 24 hr, and peak CK-MB values had to be twice more than the cutoff (<20 mU/ml).

Statistic Analysis

All continuous variables were expressed as means ± SD and categorical data as absolute values and percent-

ages. Unpaired Student's t-test with chi-square and Fisher exact tests were used to compare differences in various parameters between PD(+) and PD(−) groups. A $p < 0.05$ was considered statistically significant. Multiple regression and stepwise regression analyses were performed to determine which factors were independently associated with the change in WMS. Variables included as independent factors were gender, age, the average time interval between CAG and the onset, peak CK-MB, LVEF, and PD.

RESULTS

A 67-year-old man with acute inferior myocardial infarction was admitted to our coronary care unit (Fig. 1). Emergent CAG was performed 6 hr after the onset. The right coronary artery was totally occluded. It was reperfused by direct PTCA, and then 25% stenosis with TIMI grade 3 flow was finally observed. Electrocardiogram (ECG)-gated Gd-DTPA–enhanced MRI was performed 11 days after the onset. PD area was seen in the subendocardial inferior wall on the image obtained 90 sec after contrast injection. The inferior wall had delayed enhancement on the image obtained 7 min after contrast injection. The delayed enhanced area was larger than the PD area.

PD was observed in 32 of 43 patients (74%). All 11 patients of the PD(−) group had TIMI grade 3 flow after reperfusion. In the PD(+) group, 12 patients had TIMI grade 2 flow and 20 patients had TIMI grade 3 flow. TIMI grade 3 flow was obtained in 31 patients. In this group, PD was detected in 77.8% of patients treated with direct PTCA and in only 28.6% of patients treated by thrombolytic therapy with or without PTCA. The time interval between CAG and the onset was similar in the PD(+) group and the PD(−) group (6.0 ± 3.9 vs. 4.8 ± 2.2 hr, not significant, t-test).

Peak CK-MB of the PD(+) group was significantly higher than that of the PD(−) group (402 ± 219 vs. 135 ± 65 mU/ml, $p = 0.0006$, t-test). LVEF by echocardiography was not significantly different in the acute phase (49.9 ± 8.6% vs. 55.2 ± 7.0%, not significant, t-test) but at 1 month after onset was significantly lower in the PD(+) group than in the PD(−) group (54.9 ± 7.4% vs. 60.1 ± 4.5%, $p = 0.0454$, t-test) (Fig. 2). Total WMS by echocardiography was not different for the acute phase (16.7 ± 5.2 vs. 17.5 ± 1.35.2, not significant, t-test) and was significantly lower in the PD(+) group than in the PD(−) group at 1 month after onset (18.3 ± 3.5 vs. 23.1 ± 2.6, $p = 0.0004$, t-test) (Fig. 3). The number of patients who had an akinetic area by echocardiog-
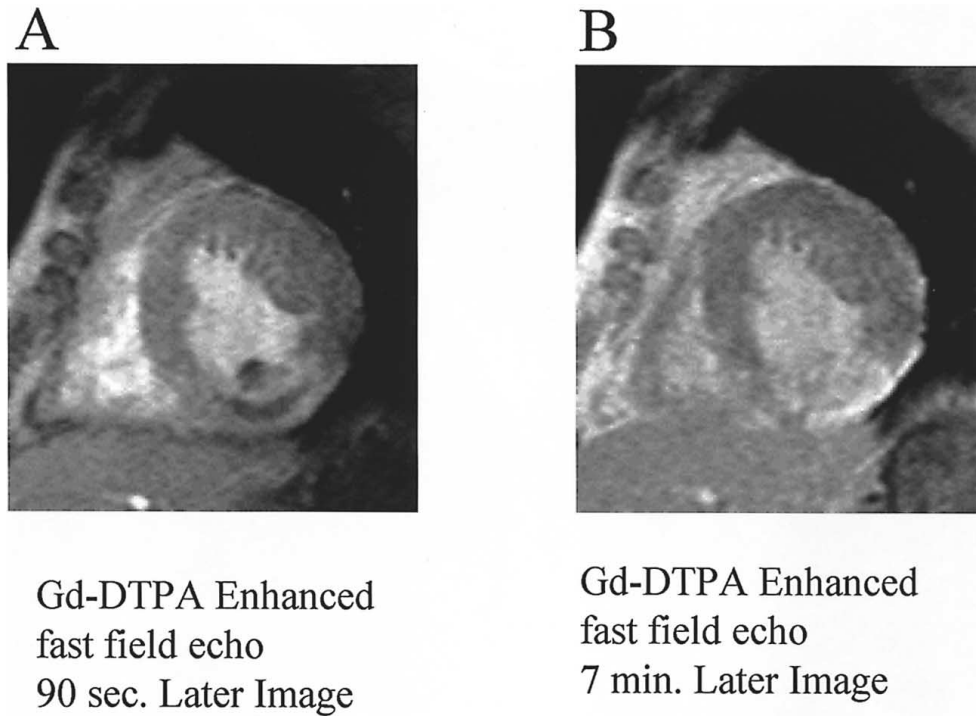
Figure 1. (A) ECG-gated Gd-DTPA–enhanced field echo MRI at 90-sec postcontrast administration. A PD area was seen in the subendocardial inferior wall of the LV short-axis MRI. (B) ECG-gated Gd-DTPA–enhanced field echo MRI at 7 min after injection. The inferior wall had delayed enhancement. The delayed enhanced inferior area was larger than the PD area at 30 sec after injection.

raphy was not significantly different on acute phase (20/28 vs. 2/8, not significant, chi-square test) but was significantly higher in the PD(+) group than in the PD(−) group at 1 month after onset (15/28 vs. 1/10, $p = 0.002$, chi-square test) (Fig. 4).

The number of akinetic areas by echocardiography was not significantly different between groups for the acute phase (54/196 vs. 23/70, not significant, chi-square test) but was significantly higher in the PD(+) group than in the PD(−) group at 1 month after onset (28/196 vs. 1/70, $p = 0.0005$, chi square test) (Fig. 5). The change
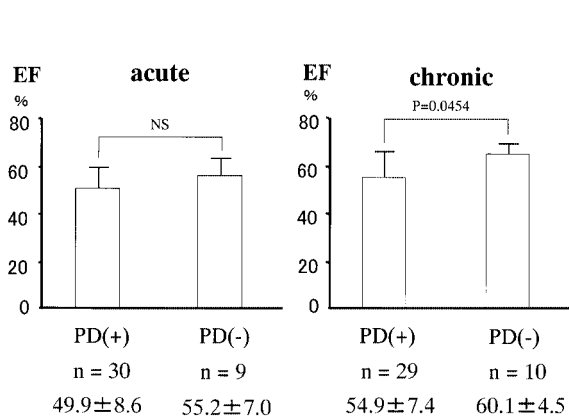

Figure 2. LVEF by echocardiography was not different in the acute phase and was significantly lower in the PD(+) group at 1 month after onset.
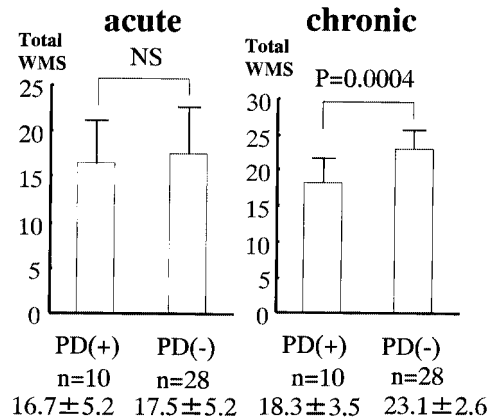

Figure 3. Total WMS by echocardiography was not different in the acute phase and was significantly lower in the PD(+) group at 1 month after onset.
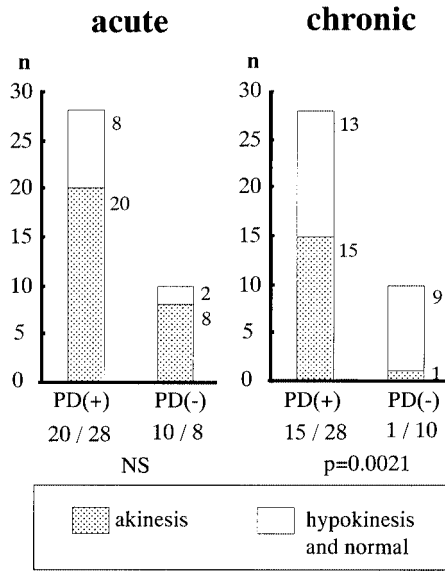
acute

chronic

Figure 4. The shaded bars show the number of patients who had akinetic areas by echocardiography. This number in the PD(+) group was not different significantly from the PD(−) group in the acute phase but was significantly higher at 1 month after onset in the PD(+) group as compared with the PD(−) group.
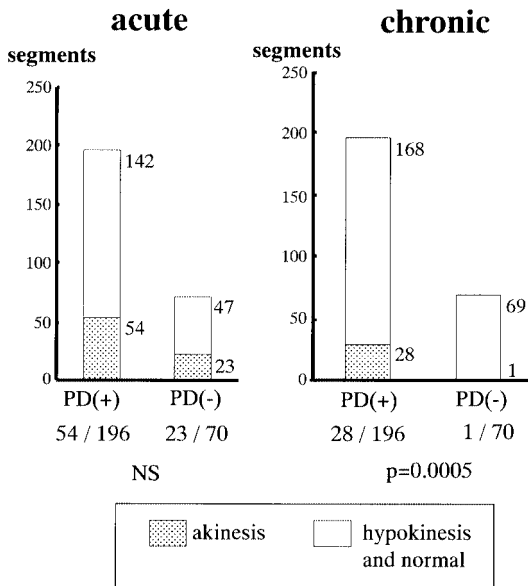
acute

chronic

Figure 5. The shaded bars show the number of segments that showed akinetic segments. This number in the PD(+) group was not different from the PD(−) group in the acute phase but was significantly higher at 1 month after onset in the PD(+) group compared with the PD(−) group.
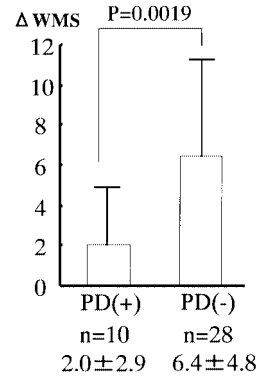

Figure 6. The change in WMS by echocardiography was significantly lower in the PD(+) group.

in WMS was significantly lower in the PD(+) group than in the PD(−) group (2.0 ± 2.9 vs. 6.4 ± 4.8, $p = 0.0019$, t-test) (Fig. 6). Results of multiple regression and stepwise regression analysis showed that PD was a significant independent factor of the change in WMS ($r = -0.703$, $p = 0.0031$). The gender, age, time interval between CAG and the onset, peak CK-MB, and LVEF were not significant independent factors of the change in WMS. The number of patients who had improvement more than two grades of WMS were 8 of 20 in the PD(+) group and 8 of 10 in the PD(−) group ($p = 0.0042$, chi-square test). The number of segments that showed more than two grades of improvement of WMS were 13 of 196 segments in the PD(+) group and 14 of 70 segments in the PD(−) group ($p = 0.0027$, chi-square test) (Fig. 7). By
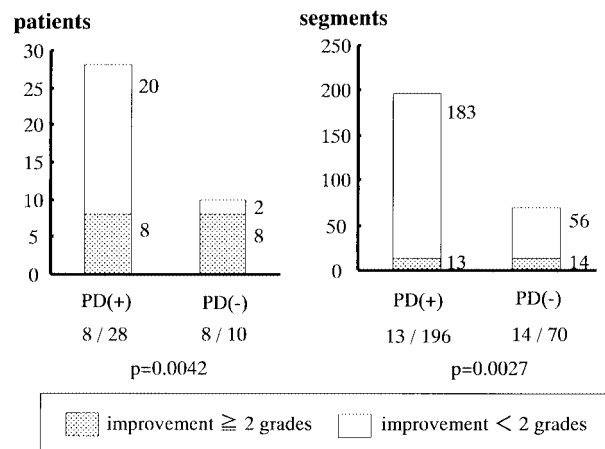

Figure 7. The number of segments that showed improvement more than two grades of WMS was significantly lower in the PD(+) group. The number of patients who had more than two grades improvement of WMS was significantly lower in the PD(+) group.
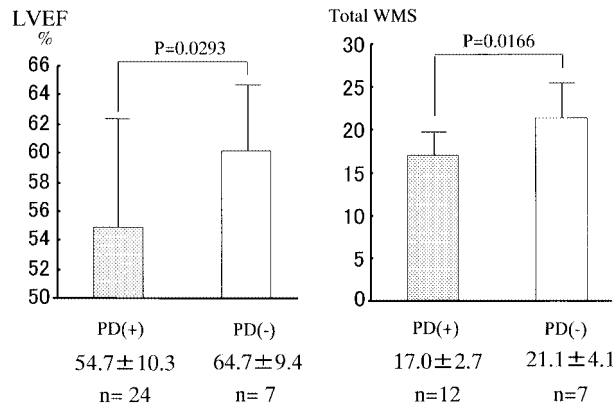
LVEF
%

P=0.0293

	PD(+)	PD(−)
	54.7±10.3	64.7±9.4
	n= 24	n= 7

Total WMS

P=0.0166

	PD(+)	PD(−)
	17.0±2.7	21.1±4.1
	n=12	n=7

Figure 8. LVEF and total WMS by LVG were significantly lower in the PD(+) group.

LVG 3 months after onset, LVEF (54.7 ± 10.3% vs. 64.7 ± 9.4%, $p = 0.0293$) and total WMS (17.0 ± 2.7 vs. 21.4 ± 4.1, $p = 0.016$) of the PD(+) group were significantly lower than those of the PD(−) group (Fig. 8).

DISCUSSION

Myocardial infarction is caused by prolonged occlusion of the epicardial coronary artery. Release of the coronary artery occlusion, if performed within the early hours after the initiation of the occlusion, restores coronary blood flow and limits infarct size. However, studies in animal models have reported that even after release of prolonged coronary artery occlusion, blood flow may not return to normal in the previously ischemic tissue. Ames et al. (23) first reported this phenomenon in the rabbit brain and termed it the no-reflow phenomenon. The no-reflow phenomenon was then observed in the canine heart by Kloner et al. (24). The no-reflow phenomenon is defined as the occurrence of areas with heterogeneous or extremely low flow after reperfusion (23).

The mechanism of the no-reflow phenomenon is not clear but is most likely a multifactorial condition established both during ischemia and at the time of reperfusion. Several mechanisms have been proposed to explain the no-reflow phenomenon. These include cell edema, microvascular damage, plugging of capillaries by red or white blood cells, and damage to endothelial cells from free radicals formed at the time of reperfusion (25–36).

Anderson et al. (37) demonstrated in the TEAM-3 study that it was difficult to distinguish angiographically between patients in whom treatment led to TIMI perfusion grade 2 at the 1-day determination of patency from patients with grade 0 or 1 perfusion by ventriculographic, enzyme, and ECG index of infarct size. In contrast, patients with grade 3 flow differed significantly from those with grade 0 or 1 and 2, suggesting that a significantly smaller infarct occurred in those patients who achieved ''complete'' perfusion. However, the no-reflow phenomenon was observed with echocardiography in not only TIMI grade 2 but also TIMI grade 3 (14).

Judd et al. (13) demonstrated a relation between MR contrast enhancement patterns and the extent and type of myocardial injury. Comparison of contrast-enhanced MR images and histologic sections showed that in hearts subjected to 90 min of left anterior descending artery occlusion followed by 48 hr of reperfusion, hypoenhanced regions were related to the no-reflow phenomenon and 90% of the myocardium within hypoenhanced regions was nonviable.

Clinically, hypoenhanced zones are characterized by large human infarcts, associated with prolonged obstruction of the infarct-related artery. On MRI, they are characterized by central dark zones surrounded by hyperenhanced regions (9,11). Microvascular obstruction occurs in humans and correlates with poorer global left ventricular function (14,15) and more frequent postmyocardial infarction complications (9,15). This has important prognostic significance after acute myocardial infarction. Myocardial contrast echocardiography (14,15,38) has correlated the presence of contrast defects with poor functional recovery of postischemic myocardium despite restored infarct-related artery flow (14,38). Unlike MRI, however, it currently requires intracoronary injection of microbubbles, necessitating cardiac catheterization in our hospital, and should be performed in the acute phase (39).

Myocardial perfusion is reduced in the hypoenhanced zone in dogs. Microvascular obstruction measured by contrast echocardiography corresponds in spatial location to microvascular obstruction by MRI and thioflavin (10). The noninvasive technique of contrast-enhanced MRI has been used to depict microvascular obstruction (11,13,16), with validation against the histopathologic standards (13,16).

Wu et al. (9) reported that the presence of MRI microvascular obstruction acutely predicted long-term prognosis in patients with myocardial infarction. But they described that infarct size did not correlate with peak creatine phosphokinase, and LVEF was similar between the PD(+) group and the PD(−) group acutely and at 6 months. They estimated global LVEF but not regional wall motion. In our study, the peak CK-MB of the PD(+) group was significantly higher than that of the PD(−) group. Infarct size was also larger in the PD(+) group.

Peak CK-MB does not describe infarct size directly, but it is considered to be a factor of infarct size. Holman et al. (40) showed that the infarct size determined by Gd-DTPA–enhanced MRI and peak CK-MB in plasma correlated significantly. Because the time interval between CAG and the onset was similar in the two groups, the peak CK-MB was estimated as the infarct size indicator in this study. Experimentally, large reperfused infarcts are more often associated with regions of no reflow than small infarctions (9,41).

Those experimental studies support the present results. In our study, LV wall contraction was estimated in detail. We evaluated not only LVEF but also regional LV wall motion. Because the LVEF and WMS assessed by echocardiography on admission did not show a significant difference between the PD(+) and PD(−) groups, accordingly the initial risk area seemed to be the same. In the PD(+) group, LVEF and WMS were worse in the chronic phase. We clinically proposed that the MRI PD was the same as the no-reflow phenomenon and the PD area was irreversible. The PD was observed in all patients of the TIMI grade 2 group and in 20 (65%) patients of the TIMI grade 3 group. Although the PD was detected in 77.8% of patients treated with direct PTCA, PDs were detected in only 28.6% of patients treated by thrombolytic therapy with or without PTCA in the TIMI grade 3 group.

Reperfusion therapy has significantly improved survival after acute myocardial infarction (42,43). However, it is difficult to gauge if ''optimal reperfusion'' has occurred (44). A ''patent'' infarct-related epicardial coronary artery by angiography is an inadequate marker of tissue-level reperfusion (14,44). The entire mechanism and treatment of no-reflow phenomenon are not clear yet, but it is suggested that microvascular embolization is related to the occurrence of no-reflow phenomenon. MRI is not available for unstable patients, because it is difficult to perform cardiopulmonary resuscitation in the MR room. Accordingly, PD observed in the subacute phase by MRI has not been used to choose reperfusion therapy. Contrast-enhanced MRI will be useful, however, to estimate the effect of reperfusion therapy and predict LV function recovery in the subacute phase.

Limitations of This Study

Although this study was retrospective and patient selection was not randomized, age, gender, site of infarction, and the average time interval between CAG and the onset were similar in the PD(+) group and the PD(−) group. Different methods of LV function and wall motion assessment (echocardiography vs. LVG) were used at different times in the study. However, many articles support that echocardiographic LV wall motion assessment is similar to LVG (19–21).

CONCLUSION

The PD was detected in a significantly larger number of patients treated with direct PTCA than those treated by thrombolytic therapy with or without PTCA in the TIMI grade 3 group. The thrombolytic therapy had an effect on the Gd-DTPA–enhanced pattern.

ACKNOWLEDGMENTS

REFERENCES

1. Frahm, J.; Merboldt, K.D.; Bruhn, H.; Gyngell, M.L.; Hanicke, W.; Chien, D. 0.3-Second Flash MRI of the Human Heart. Magn. Reson. Med. **1990**, *13*, 150–157.

2. Manning, W.; Atkinson, D.; Grossman, W.; Paulin, S.; Edelman, R. First Pass Nuclear Magnetic Resonance Imaging Studies of Patients With Coronary Artery Disease. J. Am. Coll. Cardiol. **1991**, *18*, 959–965.

3. Van Rugge, F.P.; van der Wall, E.E.; van Dijikman, P.R.M.; Louwerenbug, H.W.; de Roos, A.; Bruschke, A.V.G. Usefulness of Ultrafast Magnetic Resonance Imaging in Healed Myocardial Infarction. Am. J. Cardiol. **1992**, *70*, 1233–1237.

4. Tscholakoff, D.; Higgins, C.B.; Sechtem, U.; McNamara, M.T. Occlusive and Reperfused Myocardial Infarcts: Effect of Gd-DTPA on ECG-gated MR Imaging. Radiology **1986**, *160*, 515–519.

5. Peshock, R.M.; Mallow, C.R.; Buja, L.M.; Nunnally, R.L.; Parkey, R.W.; Willerson, J.T. Magnetic Resonance Imaging of Acute Myocardial Infarction: Gadolinium Diethylenetriamine Pentaacetic Acid as a Marker of Reperfusion. Circulation **1986**, *74*, 1434–1440.

6. Wolfe, C.L.; Moseley, M.E.; Wikstrom, M.G.; Sievers, R.E.; Wendeland, M.R.; Dupon, J.W.; Finkbeiner, W.E.; Lipton, M.J.; Parmley, W.W.; Brasch, R.C. Assessment of Myocardial Salvage After Ischemia and Reperfusion Using Magnetic Resonance Imaging and Spectroscopy. Circulation **1989**, *80*, 969–982.

7. Schaeffer, S.; Malloy, C.R.; Katz, J.; Parker, R.W.; Buja, M.; Willerson, J.T.; Peshock, RM. Gadolinium-DTPA-enhanced Nuclear Magnetic Resonance Imaging of Reperfused Myocardium: Identification of the Myocardial Bed at Risk. J. Am. Coll. Cardiol. **1988**, *12*, 1064–1072.

8. Saeed, M.; Wagner, S.; Wendland, M.F.; Derugin, N.; Finkbeiner, W.E.; Higgins, C.B. Occlusive and Reperfused Myocardial Infarcts: Differentiation With Mn-DPDP-enhanced MR Imaging. Radiology **1989**, *172*, 59–64.

9. Wu, K.C.; Zerhouni, E.A.; Judd, R.M.; Lugo-Olivieri, C.H.; Barouch, L.A.; Schulman, S.P.; Blumenthal, R.S.; Lima, J.A.C. Prognostic Significance of Microvascular Obstruction by Magnetic Resonance Imaging in Patients With Acute Myocardial Infarction. Circulation **1998**, *97*, 765–772.

10. Wu, K.C.; Kim, R.J.; Bluemke, D.A.; Rochitte, C.E.; Zerhouni, E.A.; Becker, L.C.; Lima, J.A.C. Quantification and Time Course of Microvascular Obstruction by Contrast-enhanced Echocardiography and Magnetic Resonance Imaging Following Acute Myocardial Infarction. J. Am. Coll. Cardiol. **1998**, *32*, 1756–1764.

11. Lima, J.A.C.; Judd, R.M.; Bazille, A.; Schulman, S.P.; Atalar, E.; Zerhouni, E.A. Regional Heterogeneity of Human Myocardial Infarcts Demonstrated by Contrast-enhanced MRI. Circulation **1995**, *92*, 1117–1125.

12. Wilke, N.; Simm, C.; Zhang, J.; Ellerman, J.; Ya, X.; Merkle, H.; Path, G.; Ludemann, H.; Bache, R.J.; Ururbi, K. Contrast-enhanced First Pass Myocardial Perfusion Imaging: Correlation Between Myocardial Blood Flow in Dogs at Rest and During Hyperemia. Magn. Reson. Med. **1993**, *29*, 485–497.

13. Judd, R.M.; Lugo-Olivieri, C.H.; Arai, M.; Kondo, T.; Croisille, P.; Lima, J.A.C.; Mohan, V.; Becker, L.C.; Zerhouni, E.A. Physiological Basis of Myocardial Contrast Enhancement in Fast Magnetic Resonance Images of 2-Day-Old Reperfused Canine Infarcts. Circulation **1995**, *92*, 1902–1910.

14. Ito, H.; Tomooka, T.; Sakai, N.; Yu, H.; Higashino, Y.; Fujii, K.; Matsuyama, T.; Kitabatake, A.; Minamino, T. Lack of Myocardial Perfusion Immediately After Successful Thrombolysis: A Predictor of Poor Recovery of Left Ventricular Function in Anterior Myocardial Infarction. Circulation **1992**, *85*, 1699–1705.

15. Ito, H.; Maruyama, A.; Iwakura, K.; Takiuchi, S.; Masuyama, T.; Hori, M.; Higashino, Y.; Fujii, K.; Minamino, T. Clinical Implications of the ''No Reflow'' Phenomenon. A Predictor of Complications and Left Ventricular Remodeling in Reperfused Anterior Wall Myocardial Infarction. Circulation **1996**, *93*, 223–228.

16. Kim, R.J.; Chen, E.L.; Lima, J.A.; Judd, R.M. Myocardial Gd-DTPA Kinetics Determine MRI Contrast Enhancement and Reflect the Extent and Severity of Myocardial Injury After Acute Reperfused Infarction. Circulation **1996**, *94*, 3318–3326.

17. Rochitte, C.E.; Lima, J.A.; Bluemke, D.A.; Reeder, S.B.; McVeigh, E.R.; Furuta, T.; Becker, L.C.; Melin, J.A. Magnitude and Time Course of Microvascular Obstruction and Tissue Injury After Acute Myocardial Infarction. Circulation **1998**, *98*, 1006–1014.

18. Chesebro, J.H.; Knatterud, G.; Roberts, R.; Borer, J.; Cohen, L.S.; Dalen, J.; Dodge, H.T.; Francis, C.K.; Hillis, D.; Ludbrook, P. Thrombolysis in Myocardial Infarction (TIMI) Trial, Phase I: A Comparison Between Intravenous Tissue Plasminogen Activator and Intravenous Treptokinase. Circulation **1987**, *76*, 142–145.

19. Fujii, J.; Sawada, H.; Aizawa, T.; Kato, K.; Onoe, M.; Kuno, Y. Computer Analysis of Cross Sectional Echocardiogram for Quantitative Evaluation of Left Ventricular Asynergy in Myocardial Infarction. Br. Heart J. **1984**, *51*, 139–148.

20. Gentile, F.; Greco, R.; Siciliano, S.; Violini, R.; Marsico, L.; Mininni, N.; Marsico, F. Comparative Accuracy of Cross-Sectional Echocardiography and Cineventriculography for Left Ventricular Evaluation After Myocardial Infarction. G. Ital. Cardiol. **1981**, *11*, 1996–2002.

21. Spinnler, M.T.; Cecchi, E.; Fubini, A.; Castellano, G.; Morello, P.; Bobbio, M.; Montemurro, D.; Mancini, E. Comparison of Two-Dimensional Echocardiography, Angiocardioscintigraphy and Cineventriculography in the Study of Left Ventricular Wall Motion in Ischemic Cardiopathy. G. Ital. Cardiol. **1988**, *18*, 456–464,

22. AHA Committee Report. A Reporting System on Patients Evaluated for Coronary Artery Disease. Circulation **1975**, *51*, 5–40.

23. Ames, A. 3d; Wright, R.L.; Kowada, M.; Thurston, J.M.; Majno, G. The No-Reflow Phenomenon. Am. J. Pathol. **1968**, *52*, 437–453.

24. Kloner, R.A.; Ganote, C.E.; Jennings, R.B. The ''No-Reflow'' Phenomenon After Temporary Coronary Occlusion in Dog. J. Clin. Invest. **1974**, *54*, 1496–1508.

25. Kloner, R.A.; Rude, R.E.; Carlson, N.; Maroko, P.R.; DeBoer, L.W.; Braunwald, E. Ultrastructural Evidence of Microvascular Damage and Myocardial Cell Injury After Coronary Occlusion: Which Comes First? Circulation **1980**, *62*, 945–952.

26. Engler, R.; Schmid Schonbein, G.W.; Pavelec, R.S. Leukocyte Capillary Plugging in Myocardial Ischemia and Reperfusion in Dog. Am. J. Pathol. **1983**, *111*, 98–111.

27. Schmid-Schonbein, G. Capillary Plugging by Granulocytes and the No-Reflow Phenomenon in the Microcirculation. Federation Proc. **1987**, *46*, 2397–2401.

28. Feinstein, S. Sonicated Echocardiographic Contrast Agents: Reproducibility Studies. J. Am. Soc. Echocardiogr. **1989**, *2*, 125–131.

29. Feinstein, S. Contrast Echocardiography in Humans. Perfusion and Anatomic Correlates. J. Am. Coll. Cardiol. **1988**, *11*, 59–65.

30. Schiller, N.B.; Shah, P.M.; Crawford, M.; DeMaria, A.; Devereux, R.; Feigenbaum, H.; Gutgesell, H.; Reichek, N.; Sahn, D.; Schnittger, I.; et al for the American Society of Echocardiography Committee of Standards, Subcommittee on Quantification of 2-Dimentional Echocardiograms. Recommendation for Quantification of Left Ventricle by 2-Dimentional Echocardiography. J. Am. Soc. Echocardiogr. **1989**, *5*, 358–367.

31. Krug, A.; Du Mesnil, R.; Korb, G. Blood Supply to the

Myocardium After Temporary Coronary Occlusion. Circ. Res. **1966**, *19*, 57–62.

32. Engler, R. Granulocytes and Oxidative Injury In Myocardial Ischemia and Reperfusion. Federation Proc. **1987**, *46*, 2395–2496.

33. Przyklenk, K.; Kloner, R.A. ''Reperfusion Injury'' by Oxygen Derived Free-Radicals? Circ. Res. **1989**, *64*, 86–96.

34. Ambrosio, G.; Becker, L.C.; Hutchins, G.M.; Weisman, H.F.; Weisfeldt, M. Reduction of Experimental Infarct Size by Recombinant Human Superoxide Dismutase: Insights into the Pathophysiology of Reperfusion Injury. Circulation **1986**, *74*, 1424–1433.

35. Mullane, K.M.; Salmon, J.A.; Kraemer, R. Leukocyte Derived Metabolites of Arachidonic Acid in Ischemia-Induced Myocardial Injury. Federation Proc. **1987**, *46*, 2422–2433.

36. Braunwald, E.; Kloner, R.A. The Stunned Myocardium: Prolonged, Postischemic Ventricular Dysfunction. Circulation **1982**, *66*, 1146–1149.

37. Anderson, J.L.; Karagounis, L.A.; Becker, L.C.; Sorensen, S.G.; Menlove, R.L. TIMI Perfusion Grade 3 but not Grade 2 Results in Improved Outcome After Thrombolysis for Myocardial Infarction: Ventriculographic, Enzymatic, and Electrocardiographic Evidence From the TEAM–3 Study. Circulation **1993**, *87*, 1829–1839.

38. Ragosta, M.; Camarano, G.; Kaul, S.; Powers, E.R.; Sarembock, I.J.; Gimple, L.W. Microvascular Integrity Indicates Myocellular Viability in Patients With Recent Myocardial Infarction: New Insights Using Myocardial Contrast Echocardiography. Circulation **1994**, *89*, 2562–2569.

39. Nishimura, T.; Kobayashi, H.; Ohara, Y. Serial Assessment of Myocardial Infarction by Using Gated MR Imaging and Gd-DTPA. AJR Am. J. Roentgenol. **1989**, *153,* 715–720.

40. Holman, E.R.; van Jongergen, H.P.W.; van Dijlman, R.M.; van der Laarse, A.; de Roos, A.; van der Wall, E. Comparison of Magnetic Resonance Imaging Studies With Enzymatic Indexes of Myocardial Necrosis for Quantification of Myocardial Infarct Size. Am. J. Cardiol. **1993**, *71*, 1036–1040.

41. Ambrosio, G.; Weisman, H.F.; Mannisi, J.A.; Becker, L.C. Progressive Impairment of Regional Myocardial Perfusion After Initial Restoration of Postischemic Blood Flow. Circulation **1989**, *80*, 1846–1861.

42. ISIS-2 (Second International Study of Infarct Survival) Collaborative Group. Randomised Trial Of Intravenous Streptokinase, Oral Aspirin, Both, or Neither Among 17,187 Cases of Suspected Acute Myocardial Infarction. Lancet **1988**, *2*, 349–360.

43. Grines, C.L.; Browne, K.F.; Marco, J.; Rothbaum, D.; Stone, G.W.; OKeefe, J.; Overlie, P.; Donohue, B.; Chelliah, N.; Timmis, G.C. A Comparison of Immediate Angioplasty With Thrombolytic Therapy for Acute Myocardial Infarction. N. Engl. J. Med. **1993**, *328*, 673–679.

44. Lincoff, A.M.; Topol, E.J. Illusion of Reperfusion. Does Anyone Achieve Optimal Reperfusion During Acute Myocardial Infarction? [Corrected and republished article originally printed in Circulation **1993**, *87*, 1792–1805.] Circulation **1993**, *88*, 1361–1374.

Request Permission or Order Reprints Instantly!

Interested in copying and sharing this article? In most cases, U.S. Copyright Law requires that you get permission from the article's rightsholder before using copyrighted content.

All information and materials found in this article, including but not limited to text, trademarks, patents, logos, graphics and images (the "Materials"), are the copyrighted works and other forms of intellectual property of Marcel Dekker, Inc., or its licensors. All rights not expressly granted are reserved.

Get permission to lawfully reproduce and distribute the Materials or order reprints quickly and painlessly. Simply click on the "Request Permission/Reprints Here" link below and follow the instructions. Visit the U.S. Copyright Office for information on Fair Use limitations of U.S. copyright law. Please refer to The Association of American Publishers' (AAP) website for guidelines on Fair Use in the Classroom.

The Materials are for your personal use only and cannot be reformatted, reposted, resold or distributed by electronic means or otherwise without permission from Marcel Dekker, Inc. Marcel Dekker, Inc. grants you the limited right to display the Materials only on your personal computer or personal wireless device, and to copy and download single copies of such Materials provided that any copyright, trademark or other notice appearing on such Materials is also retained by, displayed, copied or downloaded as part of the Materials and is not removed or obscured, and provided you do not edit, modify, alter or enhance the Materials. Please refer to our Website User Agreement for more details.

Order now!

Reprints of this article can also be ordered at
http://www.dekker.com/servlet/product/DOI/101081JCMR100107472